Contribution from the Department of Chemistry, Northwestern University,
Evanston, Illinois 60201

The Halogen to Sulfur Dioxide Bond. Structure of Iodo(sulfur dioxide)methylbis(triphenylphosphine)platinum, $Pt(CH_3)(PPh_3)_2I-SO_2$

MICHAEL R. SNOW[1] and JAMES A. IBERS*

Received May 15, 1972

The adduct $Pt(CH_3)(PPh_3)_2I-SO_2$ crystallizes from a benzene solution of the metal complex saturated with sulfur dioxide. Its crystal structure has been determined from 3143 independent reflections collected by counter methods. The yellow crystals are triclinic, space group $P\bar{1}$, with a reduced cell of $a = 11.853$ (6) Å, $b = 16.610$ (9) Å, $c = 9.738$ (5) Å, $\alpha = 98.12$ (2)°, $\beta = 108.17$ (1)°, $\gamma = 69.90$ (2)°, and $Z = 2$. The absorption corrected data gave a conventional R factor of 0.027 on full-matrix least-squares refinement. The $Pt(CH_3)(PPh_3)_2I$ portion of the molecule has triphenylphosphine groups trans to one another. The iodine atom forms a weak bond to sulfur (3.391 (3) Å) which is shorter by 0.4 Å than the van der Waals radii sum (3.80 Å), though much longer than expected for a single covalent bond (2.37 Å). The angle O-S-O is 116.1 (5)° and the I-S vector makes an angle of 21.3 (5)° with the normal to the SO_2 plane. By comparisons of infrared spectra and molecular geometry this adduct is shown to be similar to adducts of sulfur dioxide with metal complexes and with amines. It is also a good model for sulfur dioxide solvates of halide salts, none of which has yet been structurally characterized. The compound $O_2S-Ir(CO)(PPh_3)_2I-SO_2$ has been prepared in which there are SO_2 attachments to both iridium and iodine.

Introduction

The reactions of organometallic complexes with sulfur dioxide have been shown to give three chief product types. The first of these[2-5] is addition to the unsaturated metal center as in the formation of $RhCl(CO)(SO_2)(PPh_3)_2$ giving an increase in coordination number from 4 to 5. Second, substitution may occur as in the uv irradiation of solutions of *trans*-$Fe(CO)_3(PEt_3)_2$ in liquid sulfur dioxide to yield $Fe(CO)_2(SO_2)(PEt_3)_2$.[6] Finally insertion of sulfur dioxide into a metal to carbon bond may occur with the formation of a $M-SO_2R$ linkage.[7] The determination of the structure of the adduct $Pt(CH_3)(PPh_3)_2I-SO_2$[8] was undertaken in anticipation of an unusual five-coordinated platinum(II) species. The structure solution in fact shows SO_2 attachment to the iodine of the platinum coordination sphere. Adducts of SO_2 with halide salts have been known since 1916 and their spectral and equilibrium properties are now well characterized.[9] No structural data have been reported, however, and this metal complex adduct serves as a good structural model for the halide complexes. In view of the interest in SO_2 reactions, a preliminary communication[10] of this work has been published.

Experimental Section

Preparations. $Pt(CH_3)(PPh_3)_2I-SO_2$. A saturated solution of $Pt(CH_3)I(PPh_3)_2$ (prepared from $Pt(PPh_3)_3$ and methyl iodide) was treated in benzene (50 ml) under air-free conditions with excess SO_2 gas and allowed to stand at 5° for 24 hr. The yellow crystals formed were used for the structure analysis. The same compound is formed when solid $PtI(CH_3)(PPh_3)_2$ is treated with excess liquid SO_2 and allowed to stand and evaporate to dryness. *Anal.* Calcd for $Pt(CH_3)(PPh_3)_2I-SO_2$: C, 48.00; H, 3.60; S, 3.46; I, 13.71. Found: C, 48.6; H, 3.5; S. 3.7; I, 13.7.

$IrI(CO)(PPh_3)_2 \cdot 2SO_2$. $IrI(CO)(PPh_3)_2$ (prepared from the chloride by substitution[11]), 0.20 g, was refluxed in benzene (15 ml) and cooled to 0° under nitrogen. The solution was saturated with SO_2 gas and shaken for 30 min. Heptane (15 ml) saturated with SO_2 was added slowly and yellow-green crystals were deposited at 5° overnight. These were collected (0.18 g), washed with benzene-heptane, air-dried, and stored under SO_2 gas. *Anal.* Calcd for $IrI(CO)(PPh_3)_2 \cdot 2SO_2$: C, 44.35; H, 3.23; S, 6.40; I, 12.67. Found: C, 44.44; H, 3.09; S, 6.67; I, 12.45.

Collection and Reduction of Intensity Data

Yellow parallelepipeds of $Pt(CH_3)(PPh_3)_2I-SO_2$ were examined by precession photography using Mo Kα radiation and tentatively assigned to the triclinic system. This assignment was confirmed on a FACS-I Picker four-circle automatic diffractometer by systematically exploring reciprocal space to find the smallest primitive cell. A Delaunay reduction of this cell followed and provided a reduced cell in conventional orientation. The lattice constants at 23° were determined from a least-squares refinement of the setting angles of 12 centered higher order reflections using Mo Kα_1 radiation (λ 0.70930 Å) obtained from a graphite monochromator. The Delaunay reduced cell constants and crystal data are $a = 11.853$ (6) Å, $b = 16.610$ (9) Å, $c = 9.738$ (5) Å, $\alpha = 98.12$ (2)°, $\beta = 108.17$ (1)°, and $\gamma = 69.90$ (2)°, $V = 1709.5$ Å^3, $d_{\text{calcd}} = 1.797$ g/cm^3, d_{obsd} was not obtained, $Z = 2$, and μ(Mo Kα_1) = 52.2 cm^{-1}. The space group $P\bar{1}$ was initially assumed and subsequently confirmed by satisfactory structure analysis.

The mosaicity of the crystal was measured by means of the narrow-source, open-counter, ω-scan technique.[12] The width at half-height for typical strong reflections was satisfactorily narrow and in the range 0.05–0.07°. The crystal was bounded by the faces $\{01\bar{1}\}$, $\{110\}$, and $\{100\}$ and the distances between these pairs were 0.171, 0.120, and 0.066 mm, respectively. The crystal was mounted on a glass fiber with the [011] reciprocal lattice vector roughly coincident with the spindle axis. The intensities were measured using Mo Kα radiation by the θ-2θ technique at scan speeds of 1 or 2°/min at a takeoff angle of 2.0°. At this angle the intensity of a reflection was about 80% of the maximum as a function of takeoff angle. A receiving counter aperture 6.5 × 6.5 mm was used and positioned 30 cm from the crystal. A nonsymmetric scan range from 0.55° below the Kα_1 peak to 0.5° beyond the Kα_2 peak was used. Stationary-counter, stationary-crystal background counts of 20 sec (out to $2\theta = 30°$) and of 40 sec (from 30 to 41.5°) were measured at each end of the scan. Attenuators were inserted automatically when the intensity of the reflection exceeded about 7000 counts/sec during the scan. The pulse height analyzer was set for 95% window, centered on the Mo Kα peak.

---

(1) On leave from the Department of Physical and Inorganic Chemistry, The University of Adelaide, Adelaide, South Australia.

(2) L. Vaska, *Accounts Chem. Res.*, 1, 335 (1968).

(3) L. Vaska and S. S. Bath, *J. Amer. Chem. Soc.*, 88, 1338 (1966).

(4) S. J. La Placa and J. A. Ibers, *Inorg. Chem.*, 5, 405 (1966).

(5) K. W. Muir and J. A. Ibers, *Inorg. Chem.*, 8, 1921 (1969).

(6) R. Burt, M. Cooke, and M. Green, *J. Chem. Soc. A*, 2645 (1969).

(7) A. Wojcicki, *Accounts Chem. Res.*, 4, 344 (1971).

(8) We have departed from IUPAC ligand order notation to show the site of attachment of the SO_2.

(9) T. C. Waddington, "Non Aqueous Solvent Systems," Academic Press, New York, N. Y., 1965, pp 256-259, and references therein.

(10) M. R. Snow, J. McDonald, F. Basolo, and J. A. Ibers, *J. Amer. Chem. Soc.*, 94, 2526 (1972).

(11) J. A. McGinnety, R. J. Doedens, and J. A. Ibers, *Inorg. Chem.*, 6, 2243 (1967).

(12) T. C. Furnas, "Single Crystal Orienter Instruction Manual," General Electric Co., Milwaukee, Wis., 1957.

Table I. Positional, Thermal,[a] and Group Parameters for $Pt(PPh_3)_2CH_3I\text{–}SO_2$

Atom	x	y	z	β_{11}[a]	β_{22}	β_{33}	β_{12}	β_{13}	β_{23}
Pt	−0.03268 (3)[b]	0.22824 (2)	0.18305 (3)	0.00488 (3)	0.00250 (1)	0.00684 (4)	−0.00099 (2)	0.00137 (3)	0.00057 (2)
I	0.08011 (5)	0.34104 (3)	0.16257 (6)	0.00726 (6)	0.00364 (3)	0.01194 (8)	−0.00224 (3)	0.00324 (5)	0.00041 (4)
S	−0.0237 (3)	0.6305 (2)	0.1936 (3)	0.0108 (3)	0.0071 (2)	0.0175 (4)	0.0002 (2)	0.0042 (3)	0.0036 (2)
P(1)	−0.2212 (2)	0.3371 (1)	0.1402 (2)	0.0048 (2)	0.0027 (1)	0.0078 (3)	−0.0011 (1)	0.0010 (2)	0.0004 (1)
P(2)	0.1562 (2)	0.1189 (1)	0.2410 (2)	0.0056 (2)	0.0027 (1)	0.0073 (3)	−0.0006 (1)	0.0016 (2)	0.0004 (1)
O(1)	−0.1332 (8)	0.6112 (5)	0.1811 (8)	0.0179 (11)	0.0095 (5)	0.0253 (15)	−0.0047 (6)	0.0084 (10)	0.0033 (7)
O(2)	−0.0174 (8)	0.7095 (6)	0.2619 (9)	0.0204 (11)	0.0093 (6)	0.0231 (14)	−0.0044 (7)	0.0055 (10)	0.0001 (7)
C	−0.1292 (7)	0.1395 (4)	0.1678 (8)	0.0076 (8)	0.0018 (3)	0.0121 (12)	0.0001 (4)	0.0042 (8)	0.0014 (5)

Group	x_c[c]	y_c	z_c	δ	ϵ	η
R(1)	−0.4559 (3)	0.2889 (2)	0.1637 (4)	−1.838 (6)	−2.100 (3)	0.730 (6)
R(2)	−0.2463 (3)	0.4979 (2)	0.3679 (3)	−1.752 (3)	−2.840 (3)	2.277 (3)
R(3)	−0.2914 (3)	0.4005 (2)	−0.1812 (4)	−3.118 (4)	2.773 (3)	−1.364 (3)
R(1′)	0.1378 (3)	−0.0462 (2)	0.3612 (4)	−0.620 (7)	−2.019 (3)	1.111 (7)
R(2′)	0.3623 (3)	0.1683 (2)	0.5122 (4)	1.177 (4)	−2.506 (3)	0.937 (4)
R(3′)	0.2806 (3)	0.0441 (2)	−0.0199 (4)	−2.497 (4)	−2.798 (3)	−1.836 (4)

[a] The form of the anisotropic thermal ellipsoid is $\exp[-(\beta_{11}h^2 + \beta_{22}k^2 + \beta_{33}l^2 + 2\beta_{12}hk + 2\beta_{13}hl + 2\beta_{23}kl)]$. [b] Standard deviations of the least significant figures are given here and in subsequent tables in parentheses. [c] x_c, y_c, and z_c are the fractional coordinates of the rigid-group centers. The angles δ, ϵ, and η (in radians) have been defined previously.[16]

The unique *hkl* reflections out to $2\theta = 41.5°$ were gathered. Beyond this point there were very few detectable reflections. The intensities of six standard reflections were measured after every 100 reflections. Five of these showed an approximately equal and linear decline of 14% during the experiment and a correction factor of $1/(1\text{-}3.58 \times 10^{-6} N)$ was applied as a function of N, the number of the reflection in the list. The remaining standard reflection had χ near 90° and was sensitive to crystal movement. It showed unequal backgrounds toward the end of the experiment because of the wing of the peak recording as background. Four reflections with χ near 90° and background ratios >2 were eliminated during processing and the remaining reflections were substantially unaffected owing to the slight crystal movement.

All data processing was carried out as previously described.[13] The value of p selected was 0.04. The data were corrected for absorption[14] and the transmission coefficients ranged from 0.48 to 0.75. A total of 3663 unique reflections were obtained of which 520 had $I < 3\sigma(I)$.

Solution and Refinement of Structure

The Patterson synthesis using data with $2\theta < 30°$ gave the Pt and I atomic positions. A Fourier synthesis based on these contributions revealed the P and S sites. The known atoms were refined by least squares, with minimization of the function $\Sigma w(|F_o| - |F_c|)^2$, where $|F_o|$ and $|F_c|$ are the observed and calculated structure amplitudes and where the weights w are taken as $4F_o^2/\sigma^2(F_o^2)$. Scattering factors and $\Delta f'$ and $\Delta f''$ dispersion corrections for Pt, I, P, and S were taken from a new tabulation.[15] This refinement of the scale factor, positional parameters, and individual isotropic thermal parameters led to a conventional R factor, $R_1 = (\Sigma||F_o| - |F_c||/\Sigma|F_o|)$, of 0.23 and a weighted R factor, $R_2 = (\Sigma w(|F_o| - |F_c|)^2/\Sigma wF_o^2)^{1/2}$, of 0.310. A subsequent difference map yielded the positions of the remaining nonhydrogen atoms. The phenyl ring carbon atoms were refined as rigid groups of D_{6h} symmetry with $d(\text{C–C}) = 1.390$ Å, as previously described.[16] The agreement factors were $R_1 = 0.043$ and $R_2 = 0.057$ at convergence of the refinement with these atoms and isotropic thermal parameters using the 3143 reflections with $F_o^2 > 3\sigma(F_o^2)$. A cycle of refinement with anisotropic thermal parameters for the nongroup atoms was carried out and the resulting structure factors were used to compute a difference map about the expected plane of the hydrogen atoms of the methyl group. The three most prominent electron density regions could be assigned to methyl hydrogens. These hydrogen sites were idealized ($d(\text{C–H}) = 1.08$ Å, ∠HCH = 109.5°) and their contributions to F_c as well as those of the phenyl hydrogens were included in subsequent cycles of refinement (B = 5.0 Å^2) as fixed contributions. After a further refinement cycle the weighting scheme was checked by plotting $\Sigma w(|F_o| - |F_c|)^2$ averaged in ranges of $|F_o|$ *vs.* $|F_o|$. This function decreased linearly with $|F_o|$ and subsequent refinement cycles employed a correction factor of $(1.5\text{–}0.047\,|F_o|)$ to $\sigma(F_o^2)$ for reflections with $|F_o| < 130$. These adjustments gave a constant value of the function $\Sigma w(|F_o| - |F_c|)^2$ and the necessity for them indicates that too large a value of p was used in assigning the standard deviations. The refinement converged with $R_1 = 0.027$ and $R_2 = 0.031$. The error in an observation of unit weight was 1.006. A final difference map showed no peaks of height greater than 0.80 (10) e/Å^3, which is approximately 20% the height of an average carbon peak in the initial difference map. The six largest peaks (range 0.6–0.8 e/Å^3) lie on C–C bonds of the phenyl rings. Of the 520 reflections omitted from refinement for which $F_o^2 < 3\sigma(F_o^2)$, eight had the ratio $|F_o^2 - F_c^2|/\sigma(F_o^2)$ in the range 3–4.

The final least-squares parameters and their standard deviations are given in Table I. The positional parameters of the ring carbon atoms which may be derived from the data of Table I are given in Table II. The idealized positions of the hydrogen atoms are given in Table III. Table IV contains the observed and calculated structure amplitudes (×10)[17] in electrons.

Results and Discussion

The structure consists of trans planar $PtI(CH_3)(PPh_3)_2$ units having a weak attachment to SO_2 *via* the iodine atom. In Figure 1 a stereoscopic view of the unit cell is shown and Figure 2 shows the molecular adduct. Figure 3 shows the important bond lengths in the adduct. Principal intramolecular distances and angles are given in Table V. The root-mean-square amplitudes of vibration along the principal axes of thermal motion for the anisotropically refined atoms are given in Table VI.

The Molecular Structure. Table V shows that the coordination to Pt is closely square with angles at Pt close to 90°. The methyl carbon however is significantly out of the best weighted least-squares plane of the atoms Pt, P(1), P(2), I, and C. The equation of this plane is $-0.9325x + 2.6194y$

---

(13) P. W. R. Corfield, R. J. Doedens, and J. A. Ibers, *Inorg. Chem.*, 6, 197 (1967).

(14) Cahen's program AGNOST for absorption corrections includes the Coppens-Leiserowitz-Rabinovich logic for gaussian integration and Cullen's logic for the De Meulenaer and Tompa analytical formulation. In addition to other local programs, the programs used were local modifications of Zalkin's FORDAP program, Busing and Levy's ORFFE function and error program, and Johnson's ORTEP II thermal ellipsoid plotting program. Our local least-squares program NUCLS, in its nongroup form, closely resembles the Busing-Levy ORFLS program.

(15) D. T. Cromer and J. T. Waber in "International Tables for Crystallography," Vol. IV, in press.

(16) S. J. La Placa and J. A. Ibers, *Acta Crystallogr.*, 18, 511 (1965).

(17) Table IV, a listing of structure factor amplitudes, will appear immediately following this article in the microfilm edition of this volume of the journal. Single copies may be obtained from the Business Operations Office, Books and Journals Division, American Chemical Society, 1155 Sixteenth St., N.W., Washington, D. C. 20036. Remit check or money order for \$3.00 for photocopy or \$2.00 for microfiche, referring to code number INORG-73-224.

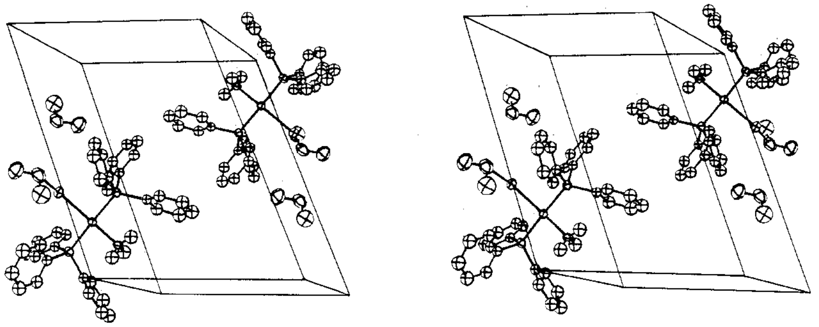

Figure 1. A stereoscopic view of the unit cell of the $Pt(CH_3)(PPh_3)_2I-SO_2$ structure. The view is approximately along z. The hydrogens of the phenyl groups have been omitted for the sake of clarity. Other atoms are drawn with 50% probability ellipsoids.

Table II. Derived Parameters for Group Carbon Atoms[a]

	x	y	z	B, Å^2
		Ring 1		
R(1)C(1)	-0.3579 (4)	0.3108 (3)	0.1472 (5)	2.5 (1)
R(1)C(2)	-0.3520 (4)	0.2871 (3)	0.2812 (4)	4.2 (2)
R(1)C(3)	-0.4500 (5)	0.2651 (4)	0.2977 (5)	5.2 (2)
R(1)C(4)	-0.5539 (4)	0.2669 (4)	0.1802 (6)	4.8 (2)
R(1)C(5)	-0.5598 (4)	0.2906 (4)	0.0462 (5)	4.7 (2)
R(1)C(6)	-0.4618 (4)	0.3126 (3)	0.0297 (4)	3.5 (2)
		Ring 2		
R(2)C(1)	-0.2325 (4)	0.4294 (2)	0.2677 (4)	2.4 (1)
R(2)C(2)	-0.1335 (3)	0.4312 (2)	0.3895 (5)	2.9 (1)
R(2)C(3)	-0.1472 (4)	0.4997 (3)	0.4897 (4)	3.4 (2)
R(2)C(4)	-0.2600 (4)	0.5664 (3)	0.4681 (5)	3.6 (2)
R(2)C(5)	-0.3591 (3)	0.5647 (3)	0.3462 (5)	3.9 (2)
R(2)C(6)	-0.3453 (4)	0.4962 (3)	0.2460 (4)	3.5 (2)
		Ring 3		
R(3)C(1)	-0.2636 (5)	0.3762 (3)	-0.0405 (4)	2.9 (1)
R(3)C(2)	-0.2750 (5)	0.3165 (2)	-0.1550 (5)	3.6 (2)
R(3)C(3)	-0.3028 (5)	0.3407 (3)	-0.2958 (4)	4.6 (2)
R(3)C(4)	-0.3192 (5)	0.4247 (3)	-0.3219 (4)	4.9 (2)
R(3)C(5)	-0.3077 (5)	0.4845 (2)	-0.2074 (5)	4.5 (2)
R(3)C(6)	-0.2799 (5)	0.4602 (3)	-0.0666 (5)	3.7 (2)
		Ring 1′		
R(1′)C(1)	0.1518 (5)	0.0227 (3)	0.3098 (5)	2.9 (1)
R(1′)C(2)	0.1732 (5)	0.0170 (3)	0.4573 (5)	3.6 (2)
R(1′)C(3)	0.1591 (5)	-0.0519 (3)	0.5087 (4)	5.0 (2)
R(1′)C(4)	0.1237 (5)	-0.1150 (3)	0.4126 (6)	5.0 (2)
R(1′)C(5)	0.1023 (5)	-0.1093 (3)	0.2651 (5)	4.6 (2)
R(1′)C(6)	0.1164 (5)	-0.0404 (3)	0.2136 (4)	3.8 (2)
		Ring 2′		
R(2′)C(1)	0.2752 (4)	0.1491 (3)	0.3903 (4)	2.7 (1)
R(2′)C(2)	0.2349 (3)	0.2055 (3)	0.4980 (5)	3.5 (1)
R(2′)C(3)	0.3220 (5)	0.2246 (3)	0.6199 (5)	4.2 (2)
R(2′)C(4)	0.4494 (4)	0.1874 (3)	0.6342 (5)	4.7 (2)
R(2′)C(5)	0.4896 (3)	0.1310 (3)	0.5265 (6)	4.6 (2)
R(2′)C(6)	0.4025 (4)	0.1119 (3)	0.4045 (5)	3.8 (2)
		Ring 3′		
R(3′)C(1)	0.2279 (5)	0.0750 (3)	0.0939 (5)	2.8 (1)
R(3′)C(2)	0.3180 (5)	-0.0055 (3)	0.1000 (5)	4.1 (2)
R(3′)C(3)	0.3707 (5)	-0.0364 (3)	-0.0138 (6)	5.1 (2)
R(3′)C(4)	0.3333 (5)	0.0131 (4)	-0.1337 (5)	5.3 (2)
R(3′)C(5)	0.2431 (5)	0.0936 (3)	-0.1397 (5)	5.5 (2)
R(3′)C(6)	0.1905 (4)	0.1245 (3)	-0.0259 (6)	3.9 (2)

[a] C(1) is attached to P; other carbon atoms are numbered successively so that C(4) is para to C(1). Ring numbering is shown in Figure 2.

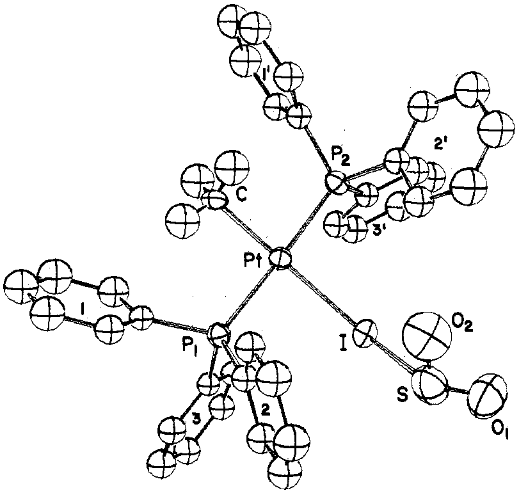

Figure 2. Structure of the $Pt(CH_3)(PPh_3)_2I-SO_2$ adduct. Phenyl hydrogen atoms are not shown.

Table III. Parameters for the Hydrogen Atoms

	x	y	z	x	y	z
		Ring 1			Ring 1′	
H(2)[a]	-0.281	0.286	0.364	0.197	0.060	0.525
H(3)	-0.446	0.249	0.392	0.173	-0.056	0.612
H(4)	-0.622	0.252	0.192	0.114	-0.163	0.448
H(5)	-0.632	0.292	-0.036	0.078	-0.153	0.198
H(6)	-0.467	0.329	-0.063	0.101	-0.037	0.111
		Ring 2			Ring 2′	
H(2)	-0.055	0.385	0.406	0.147	0.232	0.489
H(3)	-0.078	0.500	0.575	0.293	0.264	0.695
H(4)	-0.270	0.613	0.537	0.509	0.201	0.718
H(5)	-0.438	0.610	0.330	0.578	0.105	0.537
H(6)	-0.414	0.496	0.161	0.431	0.073	0.331
		Ring 3			Ring 3′	
H(2)	-0.265	0.258	-0.139	0.346	-0.040	0.183
H(3)	-0.312	0.299	-0.375	0.435	-0.092	-0.008
H(4)	-0.339	0.442	-0.419	0.370	-0.008	-0.212
H(5)	-0.319	0.543	-0.225	0.216	0.128	-0.224
H(6)	-0.272	0.502	0.012	0.127	0.180	-0.032
		Methyl Group				
H(1)	-0.098	0.088	0.105			
H(2)	-0.221	0.166	0.124			
H(3)	-0.115	0.119	0.267			

[a] Atom H(n) is attached to carbon atom C(n).

$+ 9.2051z + 2.3161 = 0$ and the deviations from it are as follows (Å): Pt, -0.0024 (3); P(1), 0.067 (2); P(2), 0.066 (2); I, -0.0010 (5); C, -0.285 (8). The sense of the displacement of the methyl group is upward from the plane of Figure 2. The orientation of the methyl group with respect to that of phenyl rings 1 and 1′ of this figure is highly suggestive that the methyl has moved up to minimize close contacts with these rings. Indeed close contacts less than the expected van der Waals distance[18] between aromatic carbon and hydrogen (2.97 Å) exist (2.41, 2.69 Å to ring 1 and 2.93, 2.85 Å to ring 1′). The triphenylphosphine groups are eclipsed with respect to each other across the platinum

(18) A. Bondi, *J. Phys. Chem.*, **68**, 441 (1964).

Table V. Selected Distances (Å) and Angles (deg)

Intramolecular Distances

Pt-I	2.707 (1)	S-O(2)	1.400 (8)
Pt-P(1)	2.300 (2)	P(1)-C	3.105 (7)
Pt-P(2)	2.310 (2)	P(2)-C	3.137 (8)
Pt-C	2.120 (7)	P(1)-C(1)[b]	1.830 (6)
I-S′[a]	3.391 (3)	P(2)-C(1)[b]	1.833 (6)
S-O(1)	1.406 (8)		

Angles

C-Pt-P(1)	89.1 (2)	O(1)-S′-I	96.9 (3)
C-Pt-P(2)	90.0 (2)	R(1)C(1)-P(1)-R(2)C(1)	98.7 (3)
C-Pt-I	172.2 (2)	R(1)C(1)-P(1)-R(3)C(1)	105.0 (3)
P(1)-Pt-P(2)	176.37 (7)	R(2)C(1)-P(1)-R(3)C(1)	108.0 (3)
P(1)-Pt-I	89.33 (6)	R(1′)C(1)-P(2)-R(2′)C(1)	101.5 (3)
P(2)-Pt-I	91.93 (6)	R(1′)C(1)-P(2)-R(3′)C(1)	102.8 (3)
Pt-I-S′	107.8 (1)	R(2′)C(1)-P(2)-R(3′)C(1)	106.7 (3)
O(2)-S-O(1)	116.1 (5)	Pt-P(1)-C(1)[b]	114.6 (3)
O(2)-S′-I	104.7 (4)	Pt-P(2)-C(1)[b]	113.8 (3)

[a] The S atom in the asymmetric unit of Table I is not the one attached to I; S′ is related to S by the operation $\bar{x}, 1 + \bar{y}, \bar{z}$.
[b] Average of three values involving the carbons bonded to P.

Table VI. Root-Mean-Square Amplitudes of Vibration (Å)

Atom	Min	Intermed	Max
Pt	0.1634 (4)	0.1719 (5)	0.1820 (5)
I	0.1801 (8)	0.2175 (8)	0.2280 (8)
S	0.224 (3)	0.261 (3)	0.346 (4)
P(1)	0.163 (3)	0.181 (3)	0.192 (3)
P(2)	0.168 (3)	0.179 (3)	0.201 (3)
O(1)	0.259 (9)	0.332 (9)	0.365 (9)
O(2)	0.315 (10)	0.340 (10)	0.349 (10)
C	0.140 (14)	0.196 (12)	0.248 (11)

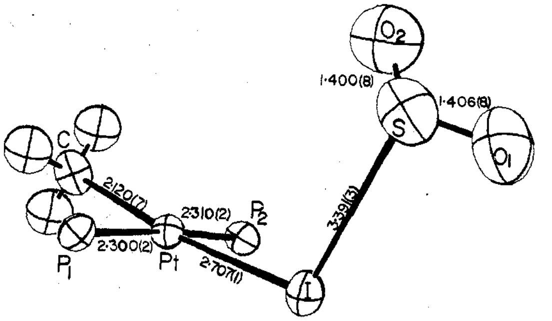

Figure 3. Coordination about Pt and I in $Pt(CH_3)(PPh_3)_2I$-SO_2 with important bond lengths.

center and this conformation is best rationalized by consideration of the relative van der Waals radii[18] of the methyl group (1.79 Å) and of iodine (1.98 Å). The iodine atom occupies the most open side of the coordination square and has only one contact to a phenyl carbon (3.67 Å to C(2) of ring 2) less than the van der Waals radii sum (3.75 Å).

The Pt-I distance, 2.707 (1) Å, is 0.06 Å longer than the sum (2.65 Å) of the Pt(II) radius[19] (1.31 Å) and half the I-I distance (1.34 Å) in solid I_2. Such an extension trans to methyl is expected by current theories of the trans effect.[20,21] An increase of 0.06 Å was found for Ir-I on going from $[IrI(NO)(CO)(PPh_3)_2][BF_4]$ (2.666(3)) to $IrI(CH_3)(NO)(PPh_3)_2$ (2.726(2) Å), where the trans ligand changes from CO to CH_3 in the basal plane of the five-coordinate complexes.[22] The Pt-P distances average 2.305 (2) Å and are in the expected range for four-coordinate Pt(II) species; thus *trans*-$Pt(H)(Cl)(PPh_2(C_2H_5))_2$ has an average Pt-P distance of 2.267 (8) Å,[23a] and *trans*-$Pt(Cl)(CO)(P(C_2H_5)_3)_2$ has the value 2.34 Å.[23b]

The most interesting part of the structure is the iodine to sulfur dioxide interaction. The I-S distance, 3.391 (3) Å, is significantly shorter than the van der Waals radii sum[18] (3.78 Å) but much longer than their single-bond radii sum 2.36 Å. It is apparent that SO_2 is acting as a weak Lewis acid in this interaction and charge transfer from iodine to SO_2 has occurred. This conclusion is supported by the electronic spectrum of the complex and by comparisons of infrared spectra and of molecular geometries within a wide range of compounds.

Spectra of SO_2 Adducts. First, adduct formation of SO_2 with halide salts is well known. The uv spectrum of $[(C_2H_5)_4N]^+I^-$-SO_2 displays a broad and intense absorption at 378 nm (ϵ ~9900) in acetonitrile solution.[24] Similar absorptions progressively shifted to higher energy are also found in spectra of the bromide and chloride salts. In fact a linear correlation of the ionization energy with the absorption energy was found in this series, in support of the charge-transfer concept. Triphenylphosphine and its metal complexes have absorptions in this region also, but the difference spectrum of the $Pt(CH_3)(PPh_3)_2I$-SO_2 complex against the SO_2-free complex at the same concentration (0.33×10^{-4} *M* in acetonitrile) has an absorption (ϵ ~15,000) which is similar to that of $[(C_2H_5)_4N]^+I^-$-SO_2 and is at the same wavelength (378 nm).

Second, the data given in Table VII show that the adduct $Pt(CH_3)(PPh_3)_2I$-SO_2 has an ir spectrum very similar to the potassium iodide solvate. The shift of the frequencies from the values of SO_2 is much smaller for these species than for O_2S-$MCl(CO)(PPh_3)_2$ (M = Ir, Rh) or O_2S-$N(CH_3)_3$, where direct metal or nitrogen to sulfur bonding has also been established by X-ray structure analysis.[4,25] In these cases a much closer approach to the sum of single-bond covalent radii (1.75 Å for N and S, 2.35 Å for Rh and S) is made by the bond lengths (Table VIII). The stronger bonds implied in these cases are consistent with the larger shifts of their S-O infrared stretching frequencies. These data provide evidence that the nature of the bonding interactions in $Pt(CH_3)(PPh_3)_2I$-SO_2 and $[I$-$SO_2]^-$ are the same. We strongly anticipate that these spectral results are insensitive to reasonable variation of the complexes to which the iodine is bonded. Thus employing the same conditions used to prepare the mono adduct O_2S-$Ir(CO)(PPh_3)_2Cl$, we have prepared the adduct O_2S-$Ir(CO)(PPh_3)_2I$-SO_2 from the corresponding iodide complex. The infrared spectrum of this species (**6**, Table VII) is nearly the sum of that of species **3** and **5** where I-SO_2 and O_2S-Ir bonds have been established by X-ray structure analysis. A preliminary communication[26] has shown that the compounds $MX(CO)(PPh_3)_2$ (M = Ir, X = Cl, Br, I; M = Rh, X = Cl) are capable of picking up gaseous SO_2 in the solid state over a temperature range of −5 to +180° at 1 atm. The maximum equilibrium amount of SO_2 taken up is with $Ir(I)(CO)(PPh_3)_2$ (2.30 mol at −5°, 1.98 mol at 25°). The compound O_2S-

---

(19) G. G. Messmer and E. L. Amma, *Inorg. Chem.*, **5**, 1775 (1966).

(20) M. R. Churchill, *Perspect. Struct. Chem.*, **3**, 91 (1970).

(21) R. Mason and A. D. C. Towl, *J. Chem. Soc. A*, 1601 (1970).

(22) D. M. P. Mingos, W. T. Robinson, and J. A. Ibers, *Inorg. Chem.*, **10**, 1043 (1971).

(23) (a) R. Eisenberg and J. A. Ibers, *Inorg. Chem.*, **4**, 773 (1965); (b) H. C. Clark, P. W. R. Corfield, K. R. Dixon, and J. A. Ibers, *J. Amer. Chem. Soc.*, **89**, 3360 (1967).

(24) E. J. Woodhouse and T. H. Norris, *Inorg. Chem.*, **10**, 614 (1971).

(25) D. Van der Helm, J. D. Childs, and S. D. Christian, *Chem. Commun.*, 887 (1969).

(26) E. C. Moroni, R. A. Friedel, and I. Wender, *J. Organometal. Chem.*, **21**, P23-P27 (1970).

Table VII. SO_2 Infrared Stretching Frequencies (cm^{-1})

No.	Compd	ν_1 sym str	ν_3 antisym str	Ref
1	SO_2 [a]	1150	1340	*f*
2	$KI \cdot 4SO_2$ [a]	1116	1294	*f*
3	$Pt(CH_3)(PPh_3)_2I-SO_2$ [a]	1138	1322	This work
4	$Pt(CH_3)(PPh_3)_2I-SO_2$ [b]	1127	1305	This work
5	$O_2S-Ir(CO)Cl(PPh_3)_2$ [b]	1057	1214, 1188[d]	2
6	$O_2S-Ir(CO)(PPh_3)_2I-SO_2$ [b]	1040, 1140[c]	1323, 1185, 1156[c,e]	This work
7	$O_2S-N(CH_3)_3$	1095	1230	*g*

[a] Acetonitrile solution. [b] Nujol mull. [c] Medium; all other peaks are strong. [d] Rhodium analog has only a single peak in this region at 1208 cm^{-1}.[5] [e] Uncertain assignment. [f] E. R. Lippincott and F. E. Welsh, *Spectrochim. Acta*, **17**, 123 (1961). [g] S. Kinumaki and T. Hata, *Ann. Gen. Chim.*, **3**, 135 (1967).

Table VIII. Geometry of SO_2 Complexes

	O_2S-RhX[a]	$O_2S-N(CH_3)_3$[b]	O_2S-IX[c]	$[O_2S-SO_2]^-$ [d]
S-Y,[e] Å	2.450 (2)	2.062 (6)	3.391 (3)	2.39 (2)
O-S-O, deg	113.8 (2)	114.8	116.1 (5)	108.0
S-O,[f] Å	1.451 (4)	1.396 (8)	1.403 (8)	1.50 (2)
α,[g] deg	30.3 (3)	22.0	21.3 (5)	15.0
Y-S-O,[f] deg	106.0 (2)	97.3	100.8[h]	98.7

[a] X = $(PPh_3)_2(CO)Cl$; ref 5. [b] Reference 25. [c] This work; X = $Pt(PPh_3)_2(CH_3)$. [d] Disodium salt; ref 31. [e] Y is the atom bonded to SO_2. [f] Average of two values given. [g] α is the angle between the S-Y vector and the normal to the SO_2 plane. [h] The values contributing to this average are 104.7 (4) and 96.9 (4)°.

$Ir(CO)(PPh_3)_2I-SO_2$, which is reported here, was analyzed after storage at room temperature under SO_2 gas and its stoichiometry is clearly in agreement with the solid-gas equilibration study. That study reports SO_2 antisymmetric stretching frequencies at 1202, 1189, and 1321 cm^{-1} for this system. The last two frequencies are in good agreement with those listed in Table VII. While the nature of the attachment of the additional SO_2 molecule was not defined in the equilibration study, it is evident from the work described here that all the species where M = Ir and X = Cl, Br, and I have halogen to SO_2 interactions. The species where M = Rh and X = Cl is reported to take up a maximum of 0.81 mol of SO_2 under the same conditions. This is remarkable as the Rh complex is isomorphous with the analogous Ir compound. The infrared spectrum shows, however, that both $Rh-SO_2$ and $Cl-SO_2$ interactions exist even though neither can be stoichiometric. When prepared from solution, the compound $O_2S-Rh(Cl)(CO)(PPh_3)_2$ can be obtained quantitatively as shown by X-ray structure analysis.[4] The equilibration data show that more SO_2 is retained in the solids to higher temperatures in the order I > Br > Cl for the $Ir(X)(CO)(PPh_3)_2$ systems. This stability sequence is the same as that derived from equilibrium studies[24] of tetraalkylammonium halides in acetonitrile.

Geometry of SO_2 Adducts. Table VIII summarizes the molecular geometry of three types of SO_2 bonding and one of the dimerization of SO_2^- in dithionite. The S-O distances are all within four standard deviations of the S-O distance in solid SO_2 (1.430 (15) Å)[27] or the value found from an electron diffraction study of the gas (1.431 (1) Å).[28] The S-O distances in $Pt(CH_3)(PPh_3)_2I-SO_2$ were averaged over thermal motion using a model in which the oxygen atom rides on sulfur. Both bond lengths increased by 0.03 Å to give a corrected average value of 1.434 (8) Å. A similar calculation was carried out for the $Pt-CH_3$ bond and only a very small increase (0.004 Å), equivalent to half a standard deviation, resulted. In view of the sensitivity of the S-O bond length to the thermal correction, no claim is made for a shortened bond length compared with the gas-state electron diffraction value. All the O-S-O bond angles presented in Table VIII, however, are significantly contracted from values determined in solid SO_2 by X-ray diffraction[27] (119.5 (1.5)°) or in the gas state by electron diffraction[28] (119.0 (5)°) and by microwave spectroscopy[29] (119.3°). The I-S vector makes an angle (α) of 21.3 (5)° with the normal to the SO_2 plane. This value is in good agreement with the comparable value of the amine adduct and near that of the dithionite ion. The value for the rhodium complex (30.3°) is larger and appears to arise from the restrictions of close intramolecular contacts. The oxygen atoms of the SO_2 molecule have contacts with the carbon atom of CO (3.068 Å) and with the (calculated) positions of the hydrogen atoms of phenyl groups (2.42, 2.65 and 2.41, 2.56 Å). The van der Waals radii[18] of hydrogen (1.20 Å), carbon (1.70 Å), and oxygen (1.50 Å) yield expected minimum approaches of 3.22 Å for C· · ·O and 2.72 Å for H· · ·O. Other intramolecular contacts with oxygen exist, such as that to a phosphorus atom (3.38 Å), which are just beyond the van der Waals radii sum (in this case 3.3 Å). A model of the complex shows that all these contacts will limit α to the vicinity of 30°. While no contacts limiting α were found in the $Pt(CH_3)(PPh_3)_2I-SO_2$ structure, the value for the $(CH_3)_3N-SO_2$ adduct cannot be much smaller. The oxygen atoms each make two intramolecular contacts with methyl groups (3.12, 3.10 and 3.13, 3.16 Å) less than the expected radii sum (3.22 Å). This discussion supports the view that the bonding to SO_2 in all these species is very similar.

The lowest unoccupied molecular orbital in SO_2 ascribed by Walsh[30] results from the out-of-phase π overlap of a p atomic orbital from each atom. It is S-O antibonding and O-O bonding and is localized mainly on the sulfur atom. Donation of a pair of electrons to this unoccupied orbital would result in a stereochemistry consistent with that seen in Table VIII. Both a lowered O-S-O bond angle from that of free SO_2 and small α values are expected qualitatively. Dunitz[31] has discussed the bonding in dithionite and he invoked the use of a dp hybrid orbital rather than a pure p molecular orbital to account for the cis conformation of dithionite ion in solid $Na_2[O_2S-SO_2]$. More recently[32] a quantitative scheme has shown for SO_2 that a 3p-3d hybrid on sulfur is the lowest unoccupied atomic orbital. This orbital has maximum overlap with a donor-pair orbital when α is 35°. Both the iodide and amine adducts have

---

(27) B. Post, R. S. Schwartz, and I. Fankuchen, *Acta Crystallogr.*, **5**, 372 (1952).

(28) J. Haase and M. Winnewisser, *Z. Naturforsch. A*, **23**, 61 (1968).

(29) Y. Morino, Y. Kikuchi, S. Saito, and E. Hiroto, *J. Mol. Spectrosc.*, **13**, 95 (1964).

(30) A. D. Walsh, *J. Chem. Soc.*, 2266 (1953).

(31) J. D. Dunitz, *Acta Crystallogr.*, **9**, 579 (1956).

(32) S. P. Ionov and M. A. Porai-Koshits, *J. Struct. Chem. (USSR)*, **7**, 245 (1966).

smaller values of α, consistent with less 3d character than was determined in that study.

Registry No. Table VII 3, 36182-31-7; 6, 36216-34-9.

Acknowledgments. We appreciate the support of this work by the National Science Foundation. M. R. S. thanks the University of Adelaide for the grant of a 1-year study leave during which time the work was carried out. We are grateful to the Matthey Bishop Co. for a donation of platinum.

Contribution from the Department of Chemistry, Northwestern University, Evanston, Illinois 60201, and Coates Chemical Laboratory, The Louisiana State University, Baton Rouge, Louisiana 70803

Reaction of Sulfur Dicyanide with $\mathrm{IrCl(CO)(PR_3)_2}$ and the Structure of Chlorocyano(thiocyanato)-*N*-carbonylbis(triphenylphosphine)iridium(III), $\mathrm{IrCl(CN)(NCS)(CO)(PPh_3)_2}$

JAMES A. IBERS,* DIANE S. HAMILTON, and W. H. BADDLEY

Received July 12, 1972

An X-ray structural determination and infrared studies of products of the reactions of sulfur dicyanide with $\mathrm{IrCl(CO)L_2}$ ($\mathrm{L = PPh_3, PMePh_2}$) have shown that $\mathrm{S(CN)_2}$ acts as a pseudohalogen in its reactions with these substrates to form *via* trans addition the cyano-*S*-thiocyanato complexes $\mathrm{IrCl(CN)(SCN)(CO)(L)_2}$. Recrystallization of these compounds from dichloromethane–methanol is accompanied by isomerization to the *N*-thiocyanato complexes. The complex $\mathrm{IrCl(CN)(NCS)(CO)(PPh_3)_2}$ crystallizes with 1 molecule in space group $C_i{}^1$-$P\bar{1}$ of the triclinic system in a reduced cell of dimensions $a = 10.141$ (5), $b = 11.222$ (5), $c = 9.381$ (6) Å; $\alpha = 112.21$ (5), $\beta = 95.02$ (5), $\gamma = 64.23$ (4)°; $\lambda(\mathrm{Cu}\ K\alpha_1)$ 1.54056 Å. The observed and calculated densities are 1.57 (3) and 1.62 g cm^{-3}. Refinement of a model with CO disordered with trans Cl and CN disordered with the NC part of the trans NCS has resulted in a conventional R factor on F of 3.2% for the 1238 counter data having $I > 3\sigma(I)$. Because of the crystallographically imposed center of symmetry, and resultant disorder, bond distances and angles are not of high precision. Important bond distances include Ir–P = 2.418 (3), Ir–Cl = 2.37 (1), Ir–C(of CO) = 1.84 (4), Ir–(C/N) = 1.99 (1), and (C/N)–S = 1.62 Å. The complex is essentially octahedral, and the N–C–S linkage is linear.

Introduction

Sulfur dicyanide, I, is an unstable, reactive molecule that has been known since 1828.[1] However, reactions of $\mathrm{S(CN)_2}$

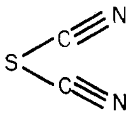

I

with transition metal complexes do not appear to have been previously investigated. In view of our earlier studies of the reactions of cyanocarbons with transition metal complexes where it was found that these strong π acids bond very effectively to electron-rich metal complexes,[2] it was of interest to investigate the reactions of cyanosulfur compounds with metal complexes. We have therefore studied the reactions of $\mathrm{S(CN)_2}$ with a number of d^8 and d^{10} noble metal substrates and describe herein the reaction of $\mathrm{S(CN)_2}$ with $\mathrm{IrCl(CO)L_2}$ ($\mathrm{L = PPh_3, PMePh_2}$) as well as the results of an X-ray study of one of the products, $\mathrm{IrCl(CN)(NCS)(CO)(PPh_3)_2}$, chlorocyano(thiocyanato)-*N*-carbonylbis(triphenylphosphine)iridium(III).

Experimental Section

Materials. The iridium complexes $\mathrm{IrCl(CO)L_2}$ were prepared according to literature procedures[3,4] as was sulfur dicyanide.[5] Because of its thermal instability, the $\mathrm{S(CN)_2}$ was stored at Dry Ice temperatures under nitrogen. Transfer of materials, reactions, and work-ups were carried out in a nitrogen atmosphere. Sulfur dicyanide has a high vapor pressure and the vapors are quite irritating to the eyes.

Reactions of Sulfur Dicyanide with $\mathrm{IrCl(CO)L_2}$. (A) Chlorocarbonylbis(triphenylphosphine)iridium(I) (0.39 g, 0.5 mmol) was dissolved in 30 ml of benzene and to the solution was added 0.4 g (5 mmol) of sulfur dicyanide at room temperature. As the clear mixture was stirred, it began after a few minutes to take on a cloudy appearance as a precipitate slowly formed. After 0.5 hr the off-white solid was collected on a filter. This product was recrystallized from dichloromethane–methanol as colorless octagonal prisms, mp >300°. *Anal.* Calcd for $\mathrm{C_{39}H_{30}ClIrN_2OP_2S}$: C, 54.19; H, 3.50; N, 3.24; P, 7.17; S, 3.70. Found: C, 53.88; H, 3.57; N, 3.27; P, 7.19; S, 4.15. The X-ray analysis described below provides unambiguous proof that this recrystallized product is not the result of direct addition of $\mathrm{S(CN)_2}$ to $\mathrm{IrCl(CO)(PPh_3)_2}$, but rather that oxidative addition has occurred to form $\mathrm{IrCl(CN)(NCS)(CO)(PPh_3)_2}$. Since mechanistically the N-bonded isomer is surprising, the preparation was repeated and both the initial product and that obtained upon recrystallization from various solvent mixtures were characterized by infrared techniques. Ir (Nujol): 2155 w (CN of Ir–CN), 2135 m (CN of Ir–SCN), 2080 vs (CO), and 440, 420 m (SCN bend). The higher value of the C–N stretching frequency, along with its sharpness (as contrasted to the lower frequency and broadness of the C–N stretch in the isomer described below), the absence of an absorption in the 760–880-cm^{-1} range which is characteristic of M–NCS bonding, and the bending frequencies in the 400–440-cm^{-1} range (which are characteristic of M–SCN bonding as contrasted to bending frequencies in the 450–490-cm^{-1} range for *N*-thiocyanates), is suggestive of an *S*-thiocyanate structure. As noted above, recrystallization of the initial *S*-bonded product from dichloromethane–methanol gives a compound which from the X-ray study is known to be the N-bonded form. Infrared data are consistent with an *N*-thiocyanato structure. Ir (Nujol): 2155 w (CN of Ir–CN), 2115 vs, br (CN of Ir–NCS), 2075 vs (CO), 875 m (CS), and 455 m (NCS bend). Both this N-bonded isomer and the S-bonded form show a strong infrared absorption at 310 cm^{-1} which is ascribed to the iridium–chlorine stretching frequency. The Raman spectra of both isomers also show a band at 310 cm^{-1}.

No isomerization occurred when the initial S-bonded form was recrystallized from a dichloromethane–tetrahydrofuran mixture; an analytically pure form of the S isomer was obtained in this manner.

---

* Address correspondence to this author at Northwestern University.

(1) M. Lassaigne, *Ann. Chim. Phys.*, 39, 197 (1828).

(2) W. H. Baddley, *Inorg. Chim. Acta Rev.*, 2, 7 (1968).

(3) K. Vrieze, J. P. Collman, C. T. Sears, and M. Kubota, *Inorg. Syn.*, 11, 101 (1968).

(4) J. P. Collman and C. T. Sears, *Inorg. Chem.*, 7, 27 (1968).

(5) D. A. Long and D. Steele, *Spectrochim. Acta*, 19, 1731 (1963).